Pre-Clinical Research Report

Journal of INTERNATIONAL MEDICAL RESEARCH

Journal of International Medical Research
2019, Vol. 47(1) 453–469

DOI: 10.1177/0300060518809255
journals.sagepub.com/home/imr
SAGE

Regulation of capillary tubules and lipid formation in vascular endothelial cells and macrophages via extracellular vesicle-mediated microRNA-4306 transfer

Ying Yang[1,*], Hui Luo[2,*], Can Zhou[1,*], Rongyi Zhang[3], Si Liu[3], Xiao Zhu[1], Sha Ke[1], Hui Liu[1], Zhan Lu[1] and Mao Chen[4]

Abstract

Objective: This study aimed to examine regulation of capillary tubules and lipid formation in vascular endothelial cells and macrophages via extracellular vesicle-mediated microRNA (miRNA)-4306 transfer

Methods: Whole blood samples (12 mL) were collected from 53 patients, and miR-4306 levels in extracellular vesicles (EVs) were analyzed by reverse transcription-polymerase chain reaction. Human coronary artery vascular endothelial cells (HCAECs) and human monocyte-derived macrophages (HMDMs) were transfected with a scrambled oligonucleotide, an miR-4306 mimic, or an anti-miR-4306 inhibitor. The direct effect of miR-4306 on the target gene was analyzed by a dual-luciferase reporter assay.

Results: EV-contained miR-4306 released from HMDMs was significantly upregulated in coronary artery disease. Oxidized low-density lipoprotein (ox-LDL)-stimulated HMDM-derived EVs inhibited proliferation, migration, and angiogenesis abilities of HCAECs *in vitro*. However, ox-LDL-stimulated HCAEC-derived EVs enhanced lipid formation of HMDMs. The possible mechanism of

[1]Department of Clinical Medicine, North Sichuan Medical College, Nanchong, China; Department of Cardiology, Affiliated Hospital of North Sichuan Medical College, Nanchong, China
[2]Department of Cardiothoracic Surgery, Nanchong Central Hospital, Nanchong, China
[3]Department of Cardiology, Nanchong Central Hospital, Nanchong, China
[4]Department of Cardiology, West China Hospital, Sichuan University, Chengdu, China

*These authors contributed equally to this work.

Corresponding author:
Mao Chen, Department of Cardiology, West China Hospital, Sichuan University, 37 Guoxue Street, Chengdu, 610041, China.
Email: treemao@sina.com

these findings was partly due to EV-mediated miR-4306 upregulation of the Akt/nuclear factor kappa B signaling pathway.
Conclusions: Paracrine cellular crosstalk between HCAECs and HMDMs probably supports the pro-atherosclerotic effects of EVs under ox-LDL stress.

Keywords
Extracellular vesicle, miR-4306, human monocyte-derived macrophage, human coronary artery vascular endothelial cell, coronary artery disease, oxidized low-density lipoprotein, lipid

Date received: 24 May 2018; accepted: 4 October 2018

Introduction

MicroRNAs (miRNAs), which are a class of small, non-coding RNAs that are approximately 21 to 25 nucleotides in length, regulate translation of mRNA and protein in plants and animals.[1] An increasing body of evidence indicates that circulating miRNAs play a pivotal role in cell-to-cell communication in coronary artery disease (CAD).[2] Endothelial release of miR126 bound to the protein argonaute 2 modulates smooth muscle gene expression and promotes a pro-atherogenic phenotype in smooth muscle cells.[3] mRNA regulatory Ago2•miRNA-223 complexes can be transported by activated platelets to endothelial cells.[4]

Extracellular vesicles (EVs) are nanovesicles of endocytic origin that are released from most cell types.[5] Circulating EVs released from erythrocytes, leukocytes, platelets, and endothelial cells carry a multitude of biological information to alter the pathophysiological processes of CAD.[6] EVs are the main extracellular vehicles for distinct miRNAs in the circulation.[7]

In this study, we investigated whether there is functional transfer of EVs and EV-derived miRNA-4306 between human monocyte-derived macrophages (HMDMs) and human coronary artery vascular endothelial cells (HCAECs).

Methods

Patients

We recruited 53 patients who underwent diagnostic coronary angiography and were admitted to our hospital between July 2015 and July 2016. Patients were classified into three groups as follows. (1) The control group comprised patients who had chest pain syndrome with normal coronary artery findings ($n = 15$). (2) The elective percutaneous intervention (PCI) group comprised patients who had PCI performed within 2 weeks ($n = 15$). (3) The emergency PCI group comprised patients who had PCI performed within 12 hours ($n = 20$) (Supplementary Table 1). The PCI groups included patients who exclusively had effort-related angina with a positive exercise stress test and at least one coronary stenosis was detected at angiography with $> 70\%$ reduction of the lumen diameter. Additionally, patients in the PCI groups had chest pain lasting for > 30 minutes within 24 hours before enrollment and a large rise in troponin I levels. A total of 20 mL of whole fasting blood samples were collected from 53 patients. HMDMs from each donor were immediately isolated from venous blood and placed in RPMI 1640

medium. The protocol was approved by the Ethics Committee of West China Hospital. Written informed consent was obtained from each patient.

Cell culture

HCAECs were purchased from the Cell Bank of the Chinese Academy of Sciences (Chengdu, China). HMDMs were isolated from donors. Briefly, monocytes were first extracted from peripheral blood samples and then allowed to adhere to cell culture plates for 4 days in RPMI 1640 medium (Sigma-Aldrich, St Louis, MO, USA) containing 10% fetal bovine serum (FBS) (Cell Culture Bioscience, Shanghai, China), 5% human AB serum (Sigma-Aldrich), antibiotics, GlutaMax (Gibco, Grand Island, NY, USA), and recombinant human macrophage colony-stimulating factor (M-CSF; PeproTech, Rocky Hill, NJ, USA). The monocytes were then resuspended in RPMI 1640 medium containing 10% FBS and further cultured for 2 days. The cell culture medium was then replaced with RPMI 1640 supplemented with 5% FBS for 1 day.

Isolation and characterization of EVs

HMDMs and HCAECs were exposed to 100 μg/mL oxidized low-density lipoprotein (ox-LDL) for 12 hours, followed by centrifugation at $400 \times g$ for 5 minutes. The cells were ultracentrifuged at $2000 \times g$ for 20 minutes to remove cellular debris. After washing of the EV pellets with phosphate-buffered saline at $110{,}000 \times g$ for 2 hours, the supernatant was ultracentrifuged at $110{,}000 \times g$ for 2 hours at 4°C. Protein content of the EVs was used to normalize for EV quantity between experiments using the Pierce microplate bicinchoninic acid protein assay kit (Thermo Fisher Scientific, USA, Rockford, IL, USA). The activation status and origin of the EV fractions were detected by flow cytometry. EVs from HMDMs or HCAECs were labelled with CD45-FITC or CD31-FITC. The samples were then detected cytofluorometrically using a flow cytometer (BD Biosciences, San Jose, CA, USA).

Fluorescence labelling of EVs and microscopy

Cultured HMDMs or HCAECs were labelled with DiI-C16 for 30 minutes. The supernatant was collected and centrifuged to isolate EVs. Human monocyte-EVs (HM-EVs/endothelial cell-EVs (EC-EVs) in the medium were incubated with HCAECs or HMDMs. After incubation for 12 hours, HMDMs or HCAECs were washed, fixed, and observed by microscopy (Olympus, Tokyo, Japan).

For electron microscopy, the EV pellet was placed in a droplet of 2.5% glutaraldehyde in phosphate-buffered saline at a pH of 7.2 and fixed overnight at 4°C. The samples were then embedded in 10% gelatin and fixed in glutaraldehyde at 4°C and cut into several blocks (<1 mm^3). The samples were dehydrated for 10 minutes for each step in increasing concentrations of alcohol (30%, 50%, 70%, 90%, 95%, and 100% $\times 3$). Samples were embedded in pure, fresh Quetol-812 epoxy resin and polymerized at 35°C for 12 hours, 45°C for 12 hours, and 60°C for 24 hours. Ultrathin sections (100 nm) were cut using a Leica EM UC7 ultra-microtome (Leica Microsystems, Beijing, China) and post-stained with uranyl acetate for 10 minutes and with lead citrate for 5 minutes at room temperature before observation with a FEI Tecnai T20 transmission electron microscope equipped with a Gatan UltraScan 894 CCD (Thermo Fisher Scientific, Waltham, MA, USA), operated at 120 kV.

Bromodeoxyuridine incorporation assay

HMDM proliferation was evaluated using a 5-Bromo-2′-deoxy-uridine Labelling and Detection Kit II (Roche, Basel, Switzerland) according to the manufacturer's instructions and manual cell counting. The absorbance of cells was detected by a microplate reader at 405 nm with a reference measurement at 490 nm. Absorbance (A 405 nm-A 490 nm) values representing cell proliferation ability were compared among treatments.

Transwell migration assay

The migration ability of HMDMs was measured in a Transwell Chamber (6.5 mm, Costar; Sigma-Aldrich). MicroRNA (mimics or inhibitor), vascular endothelial growth factor A (VEGFA) small interfering RNA, HCAEC-derived EVs, and/or their respective controls were transfected into HMDMs. Transfected cells were cultured in Dulbecco's modified Eagles medium (DMEM) supplemented with 0.5% serum for 24 hours and harvested by trypsinization. An aliquot (250,000 cells/200 μL) of the cells in serum-free DMEM was dispensed into the transwell inserts (8-mm pore size) that were precoated with 0.5% gelatin (G1393; Sigma-Aldrich), and DMEM (600 μL) with 20% FBS was placed in the lower chamber. The transwell plates were incubated at 37°C in a 5% CO_2 incubator for 18 to 24 hours. Cells remaining on the upper surface of the filter membrane (nonmigrant) were gently scraped off with a cotton swab. Images of migrant cells were captured by a photomicroscope (BX51; Olympus). Cell migration was quantified by blind counting of the migrated cells on the lower surface of the membrane, with five fields per chamber.

Capillary tube formation assay

Briefly, at least 30 minutes before the experiment, each well of a 24-well plate was coated with 100 μL of Matrigel (BD Biosciences) at 37°C. HCAECs were pretreated in the presence of HMDM EVs (20 μg of total protein per well) or a saline solution in starvation medium at 37°C for 24 hours. HCAECs were seeded onto the plated Matrigel at a concentration of 1×10^5 cells/well, and each treatment was repeated in three wells. After 6 hours, images of formation of capillary-like structures were examined under a light microscope (Olympus) at 200× magnification.

Transfection and vector construction

MicroRNAs (mimics or inhibitors) (Invitrogen, Carlsbad, CA, USA) and small interfering RNAs were transfected using Lipofectamine 2000 (Invitrogen). Lentiviral expression constructs of miR-4306 and negative control lentiviruses (Invitrogen) were purchased. VEGFA expression by lentivirus was constructed by inserting the VEGFA open reading frame into the pLenti6.3 vector (Invitrogen). Lentiviral infection was performed according to the manufacturer's instructions.

Plasmid construction and luciferase assay

The DNA sequence of the entire human VEGFA 3′-UTR was amplified by polymerase chain reaction (PCR). The amplified DNA sequences were inserted into the p-MIR-report plasmid (Sangon Biotech, Shanghai, China). For luciferase reporter assays, 293T cells were cotransfected with an individual reporter gene (pmiR-Luc-VEGFA-WT, pmiR-Luc-VEGFA-MUT1, or pmiR-Luc-VEGFA-MUT2), a control, or miR-4306 mimics using TransIT-X2 transfection reagent (Invitrogen).

The pGL4.74(hRluc/TK) plasmid, a control luciferase plasmid, and the pGL4.32(luc2P/NF-κB-RE/Hygro) plasmid (Invitrogen) were transfected using Lipofectamine 2000 reagent (Sangon Biotech). A Renilla plasmid (Invitrogen) was used as an internal control for all transfection assays. After transfection for 48 hours, the activities of luciferase and Renilla were tested using a standard protocol (Sangon Biotech).

RNA isolation and quantitative reverse transcription-PCR

Total RNA isolation from HM-EVs and EC-EVs was performed using TRIzol reagent (Invitrogen), and isolation from the supernatant fraction was performed using an mirVana PARIS kit (Invitrogen). A total of 1 mg of RNA was reversely transcribed into cDNA (TaKaRa Biotechnology Ltd., Dalian, China) after DNase I treatment (Invitrogen). MicroRNA-4306 was detected by quantitative reverse transcription (qRT)-PCR using a miScript Primer Assay kit and SYBR Green (Qiagen, Dusseldorf, Germany). Small nuclear RNA U6 (RNU6) was used as a reference gene with the following primers: RNA U6 primers, forward — 5′-CTCGCTTCGGCAGCACA-3′ and reverse — 5′-AACGCTTCACGAATTTGCGT-3′; and miR-4306 RT primer, 5′-CTCAACTGGTGTCGTGGAGTCGGCAATTCAGTTGAGGGTACAGA-3′. The forward primer 5′-GCCGAGAAGCUGCUUAGUGU-3′ and reverse primer 5′-CTCAACTGGTGTCGTGGA-3′ were also used. The following program was used: 10 minutes of initial denaturation and enzyme activation at 95°C, followed by 40 cycles composed of 15 s at 95°C, 15 s at 60°C for annealing, and 15 s at 72°C for elongation. Subsequently, for the melting curve, a program of 5 s at 95°C, 1 s at 25°C, 15 s at 70°C, and 1 s at 95°C was used. During the qRT-PCR assays, a no reverse transcriptase control sample was used to evaluate PCR amplification of contaminating genomic DNA. Each experiment was conducted three times. The relative gene expression was quantified using the $2^{-\Delta\Delta Ct}$ method.[8]

Western blotting analysis

Total protein extracts were isolated from the cell suspension. Proteins from each sample were separated by sodium dodecyl sulfate-polyacrylamide gel electrophoresis and were transferred onto a nitrocellulose membrane (Millipore, Bedford, MA, USA). Proteins were tested by primary antibodies against VEGFA (Santa Cruz Biotechnology, Santa Cruz, CA, USA), Akt (Cell Signaling Technology, Danvers, MA, USA), phospho-Akt (Cell Signaling Technology), glyceraldehyde-3-phosphate dehydrogenase (Cell Signaling Technology), and the appropriate horseradish peroxidase-conjugated secondary antibodies. Proteins were visualized with the Enhance chemiluminescence kit (Thermo Fisher Scientific). Quantitative data were analyzed by Image-pro Plus analysis software (Chicago, IL, USA).

Cholesterol content analysis

HMDMs were stained with oil red O (ORO) and hematoxylin following a routine procedure. HMDMs with a lipid droplet area of more than the width of the nucleus were defined as ORO-positive (ORO+).

The components of lipoprotein, free cholesterol (FC), and total cholesterol (TC) in high-performance liquid chromatography were recorded continuously over time. Cholesterol ester (CE) was calculated by subtraction of FC from TC. Briefly, HMDMs were sonicated and lysed and proteins and triglycerides were removed from

HMDM lysates. FC was extracted after being dissolved in a solution of isopropanol and n-hexane (1:4, V/V). TC was obtained from an aliquot sample that was treated with cholesterol esterase. Samples were dissolved in a mobile phase containing acetonitrile: isopropanol: n-heptane (52: 35: 12, V/V). A chromatography system (VARIAN Prostar 210; Carlsbad, CA, USA) was used to analyze TC and FC levels.

Statistical analysis

All data were analyzed using SPSS for Windows, Version 16.0 (SPSS Inc., Chicago, IL, USA). The data are presented as the mean ± standard deviation of three independent experiments. Analysis of variance was used for comparisons. A value of $p < 0.05$ was considered significant.

Results

Patients' characteristics

The mean (standard deviation) age of the patients was 60.2 ± 10.2 years and 54% were men and 46% were women.

HM-EVs from patients with CAD show a reduced capacity for promoting angiogenesis in HCAECs compared with those from controls

To examine whether HMDMs secrete EVs that are taken up by HCAECs, a predominant population of EVs derived from HMDMs (HM-EVs) with leukocyte glycoprotein CD45 surface expression was found to be of monocyte origin by flow cytometry (Figure 1A). Confocal analysis showed that the HCAECs took up membrane-labelled EVs (Figure 1B-a, b). Electron microscopy showed that the separated EVs appeared as a cluster of vesicles of 30 to 100 nm in diameter and were swallowed by HCAECs (Figure 1C-a, b).

Proliferation, migration, and angiogenesis capabilities of HCAECs treated with HM-EVs that were isolated from patients with CAD were compared with those from the control group (Figure 2A–D, E-d–f, F-e–g). Proliferation of HCAECs that were treated with HM-EVs isolated from patients who had emergency PCI and those with elective PCI was significantly attenuated compared with those from the control group ($p < 0.05$ and $p < 0.01$, respectively, Figure 2A-B). The migration rates of HCAECs that were treated with HM-EVs isolated from patients who had emergency PCI and those with elective PCI were significantly lower than those from the control group ($p < 0.05$ and $p < 0.05$, respectively, Figure 2C, 2E-d–f). Tube formation of HCAECs that were treated with HM-EVs isolated from patients who had emergency PCI and those with elective PCI was significantly suppressed compared with those from the control group ($p < 0.05$ and $p < 0.01$, respectively, Figure 2D, 2F-e–g). Furthermore, HM-EVs from patients with emergency PCI showed a significantly reduced capacity for promoting angiogenesis in HCAECs compared with those from patients with elective PCI (Figure 2D, F-e–g, $p < 0.05$). We also observed that expression of HM-EV-derived miR-4306 was higher in patients with CAD compared with the control group ($p < 0.05$). Moreover, miR-4306 showed higher levels in HM-EVs from patients with emergency PCI than in those from patients with elective PCI (Figure 1D, $p < 0.05$).

EVs from ox-LDL-stimulated HMDMs reduce proliferation, migration, and capillary tubule formation of HCAECs by upregulation of nuclear factor kappa B

To determine the effects of HM-EVs on HCAEC activation, HCAECs were incubated with ox-LDL-stimulated HM-EVs.

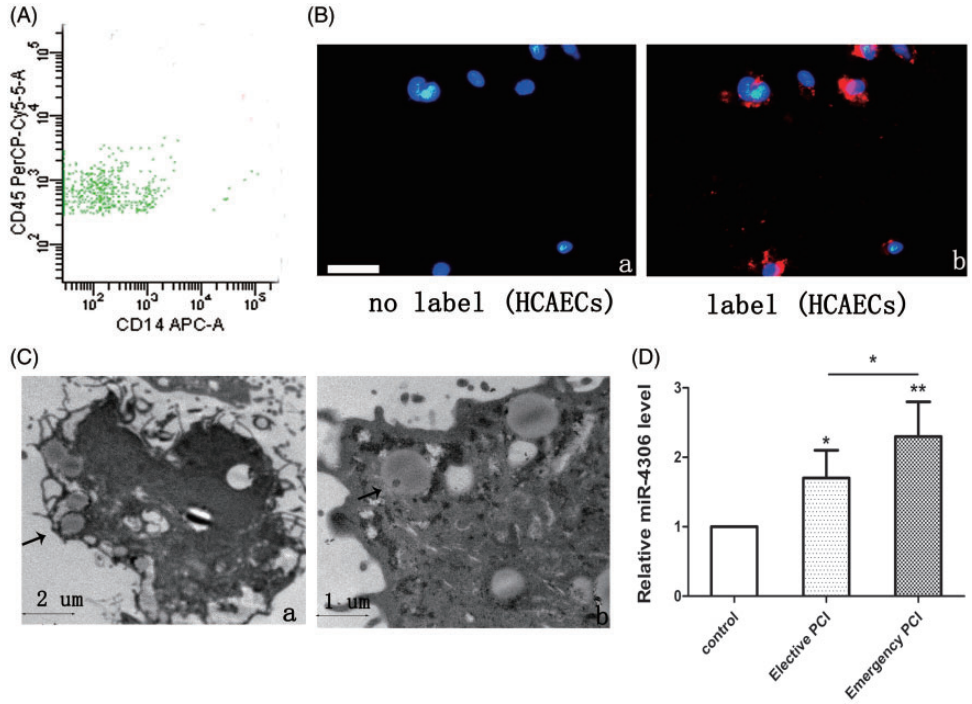

Figure 1. EVs from patients' HMDMs were taken up by HCAECs. (A) Representative flow cytometry analyses of the EV population derived from HMDMs. (B) Fluorescently-labelled EVs entering HCAECs. Fluorescently-labelled HM-EVs were incubated with HCAECs for 0 (a) or 12 hours (b) at 37°C. Original magnification, ×100; scale bar, 50 μm. (C) Electron microscopy shows that HCAECs (a, b) engulf HM-EVs (arrows). (D) Levels of miR-4306 in HM-EVs in control patients, elective patients, and emergency patients ($n = 4$). *$p < 0.05$, **$p < 0.01$. EV: extracellular vesicle; HM: human monocyte; HMDMs: human monocyte-derived macrophages; HCAECs: human coronary artery vascular endothelial cells; miRNA: microRNA.

We found that proliferation, migration, and angiogenesis abilities of HCAECs treated with ox-LDL-stimulated HM-EVs were attenuated compared with those treated with HM-EVs from unstimulated HMDMs (Figure 2A–D, E-a–c, F-a–c). We further tested whether HM-EVs had an effect on activity of a nuclear factor kappa B (NF-κB)-dependent luciferase reporter. We found that ox-LDL-stimulated HM-EVs to HCAECs increased basal and ox-LDL-stimulated activity of the reporter (Figure 3A). We then assessed whether the effects of HM-EVs could be repeated by inhibiting NF-κB signaling. Induction of proliferation, migration, and capillary tubule formation in ox-LDL-stimulated HCAECs was enhanced by the IκB kinase (IKK) inhibitor 2-[(aminocarbonyl)amino]-5-[4-fluorophenyl]-3-thiophenecarboxamide (TPCA-1) (Supplementary Figure 1).

Ox-LDL-stimulated HCAEC-derived extracellular vesicles (EC-EVs) promote HMDM lipid accumulation by upregulation of NF-κB

In flow cytometry, surface expression of glycoprotein CD61 on isolated EVs from HCAEC culture medium showed the vascular endothelial cell origin of these

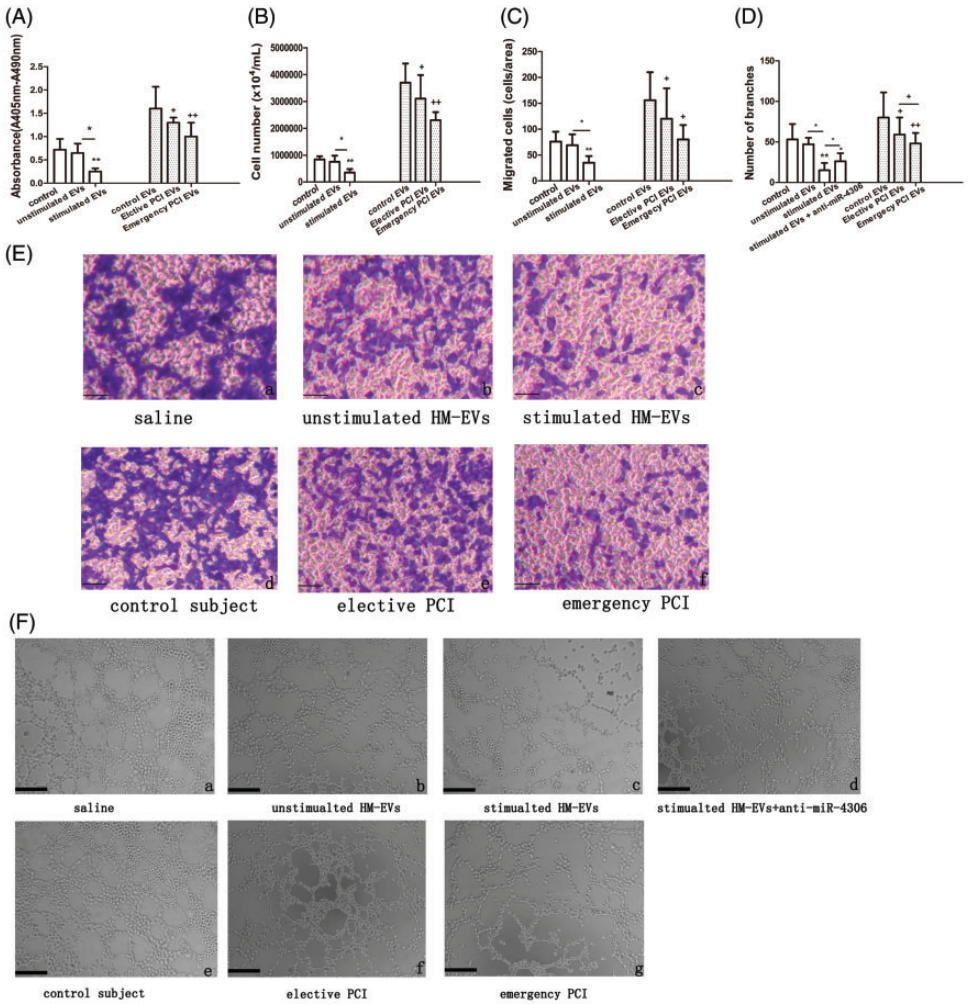

Figure 2. HM-EVs inhibited proliferation, migration, and capillary tubule formation of HCAECs. HCAECs treated with saline, non-ox-LDL-stimulated HM-EVs, ox-LDL-stimulated HM-EVs, and HM-EVs from control patients, patients with emergency PCI, or patients with elective PCI who underwent bromodeoxyuridine incorporation assays (A), cell counting (B), transwell analysis (C, E), or capillary tube formation assay (D, F). Scale bar, 100 μm (n = 4). *$p < 0.05$, **$p < 0.01$, $^{+}p < 0.05$, $^{++}p < 0.01$. EV: extracellular vesicle; HM: human monocyte; EV: extracellular vesicle; ox-LDL: oxidized low-density lipoprotein; PCI: percutaneous intervention; HCAECs: human coronary artery vascular endothelial cells.

EVs (Figure 4A-a, b). We then marked EC-EVs with DiI-C16 and tested the localization of fluorescent EC-EVs in HMDMs after incubation (Figure 4B-c, d). Under electron microscopy, isolated EVs were approximately 50 to 300 nm in size and were engulfed by HMDMs (Figure 4C-c, d).

To examine the effects of EC-EVs on HMDM lipid accumulation, we directly viewed the lipoprotein content in HMDMs when treated with 100 μg/mL ox-LDL in the

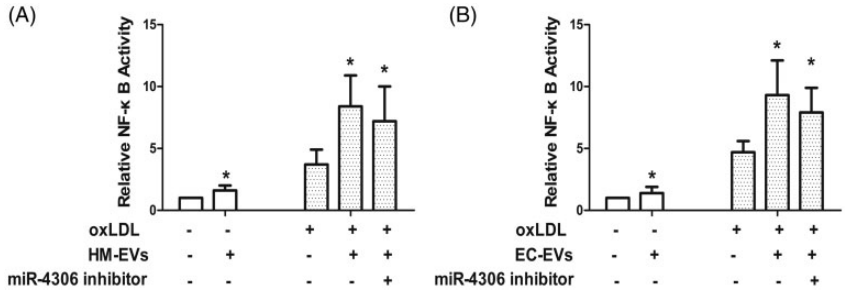

Figure 3. HM-EVs (A) and EC-EVs (B) stimulated by ox-LDL enhanced ox-LDL-stimulated activity of the NF-κB-dependent luciferase reporter (n = 3). *$p < 0.05$. EV: extracellular vesicle; HM: human monocyte; ox-LDL: oxidized low-density lipoprotein; NF-κB: nuclear factor kappa B.

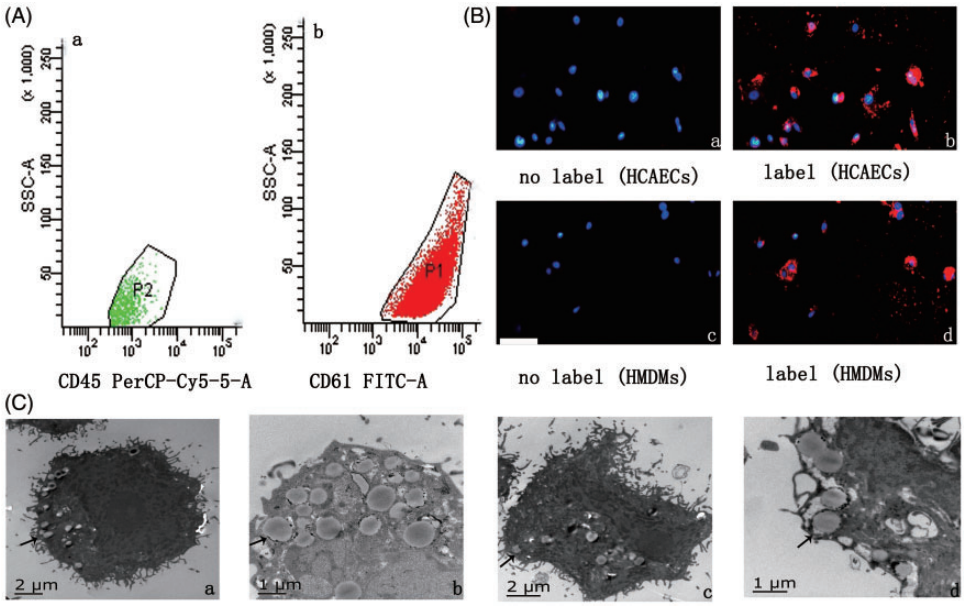

Figure 4. EVs from cells were taken up by target cells. (A) Representative flow cytometry analyses of the EV population derived from (a) HMDMs activated with 100 μg/mL ox-LDL or (b) HCAECs activated with 100 μg/mL ox-LDL. (B) Fluorescently-labelled EVs entering target cells. Fluorescently-labelled HM-EVs/EC-EVs were incubated with HCAECs/HMDMs for 0 (a, c) or 12 hours (b, d) at 37°C. Original magnification, ×100; scale bar, 50 μm. (C) Electron microscopy shows that HCAECs (a, b)/HMDMs (c, d) engulf HM-EVs/EC-EVs (arrows) (n = 4). EV: extracellular vesicle; HM: human monocyte; HMDMs: human monocyte-derived macrophages; ox-LDL: oxidized low-density lipoprotein; HCAECs: human coronary artery vascular endothelial cells.

presence of EVs isolated from HCAECs by ORO staining. Lipid droplets increased when HMDMs were treated with 100 μg/mL ox-LDL alone (Supplementary Figure 2A, B, D, $p < 0.01$ versus no ox-LDL treatment). Lipid droplets in HMDMs treated with EC-EVs that were isolated from ox-LDL-stimulated HCAECs

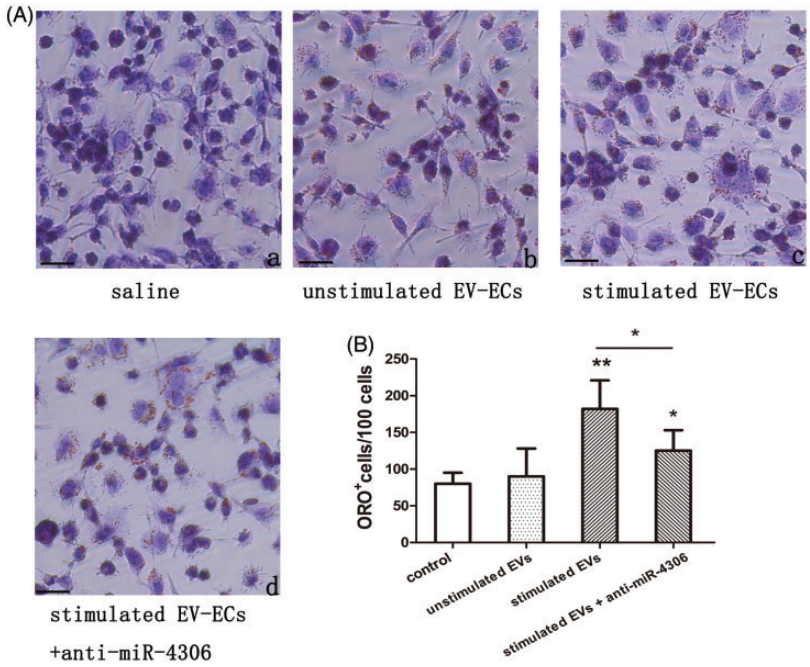

Figure 5. Effect of EC-EVs on cellular cholesterol content in HMDMs exposed to 100 μg/mL ox-LDL. HMDMs were treated with saline, non-ox-LDL-stimulated EC-EVs, ox-LDL-stimulated EC-EVs, and ox-LDL-stimulated EC-EVs plus miR-4306 inhibitor (anti-miR-4306). Intracellular lipid droplets were observed by ORO staining. Lipid droplets were stained red and nuclei were stained blue (A). ORO+ cells were counted. (B) The number of ORO+ cells in each group. Scale bar, 100 μm (n = 4). *$p < 0.05$, **$p < 0.01$. EC-EVs: endothelial cell-extracellular vesicles; HMDMs: human monocyte-derived macrophages; ox-LDL: oxidized low-density lipoprotein; miRNA: microRNA; ORO: oil red O.

(ox-LDL-stimulated EC-EVs) were significantly higher compared with those treated with HM-EVs that were isolated from unstimulated HCAECs (Figure 5A-a–c, $p < 0.01$). Similar trends were observed in ORO+ cells (Figure 5B, $p < 0.01$). Moreover, we examined the effects of EC-EVs on lipid levels in HMDMs that were exposed to ox-LDL using high-performance liquid chromatography. We observed significantly higher FC, CE, and TC levels in HMDMs in the presence of ox-LDL-stimulated EC-EVs compared with those from unstimulated EC-EVs (Table 1, all $p < 0.05$).

We also found that HMDMs exposed to EC-EVs promoted basal and ox-LDL-stimulated activity of the NF-kB-dependent luciferase reporter (Figure 3B, both $p < 0.05$). Lipid accumulation in HMDMs exposed to ox-LDL was inhibited by the IKK inhibitor TPCA-1 compared with those treated with ox-LDL alone (Supplementary Figure 2, Supplementary Table 2, $p < 0.05$).

HM-EVs/EC-EVs transfer miRNA-4306 to target HCAECs/HMDMs

Several independent approaches were used to confirm that miR-4306 could be transferred directly to HCAECs and HMDMs. First, we observed markedly higher miR-4306 levels in HCAECs and HMDMs

Table 1. Effect of EC-EVs or miR-4306 on TC, FC, and CE in HMDMs exposed to 100 μg/mL ox-LDL.

(mg/dL)	Control	Unstimulated EC-EVs	Stimulated EC-EVs	miRNA control	miR-4306
TC	155.3 ± 24.4	165.1 ± 38.9	$225.6 \pm 76.2^{*,\#}$	195.39 ± 58.1	$267.42 \pm 32.1^{+}$
FC	141.3 ± 15.6	149.5 ± 25.9	$231.1 \pm 19.5^{*,\#}$	72.65 ± 29.8	$139.42 \pm 12.8^{+}$
CE	123.1 ± 28.7	119.3 ± 35.4	$193.1 \pm 25.7^{**,\#}$	49.58 ± 19.5	$126.31 \pm 31.2^{++}$

Data represent mean ± standard deviation (n = 3). $^{*}p < 0.05$, $^{**}p < 0.01$ versus control (HMDMs exposed to oxidized low-density lipoprotein plus saline); $^{\#}p < 0.05$ versus unstimulated EC-EVs; $^{+}p < 0.05$, $^{++}p < 0.01$ versus miRNA control. FC: free cholesterol; TC: total cholesterol; CE: cholesterol ester; HMDMs: human monocyte-derived macrophages; EC-EVs: endothelial cell-extracellular vesicles; miRNA: microRNA.

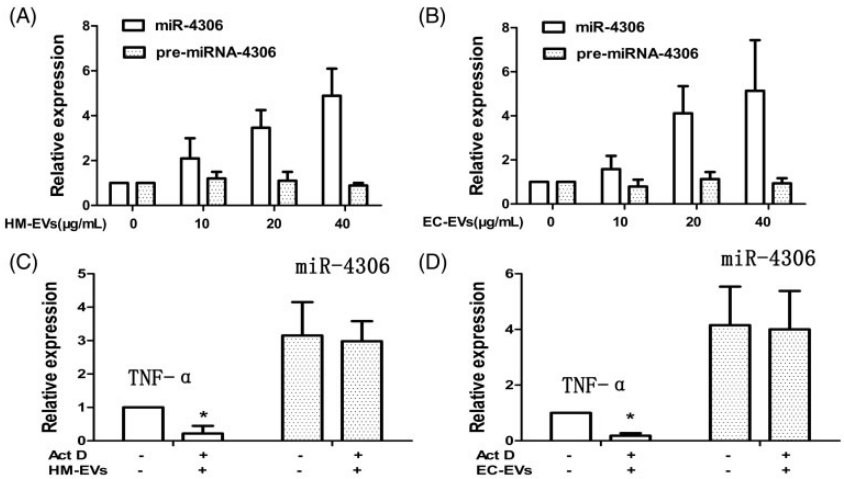

Figure 6. MicroRNA-4306 in EVs was transferred between HCAECs and HMDMs. (A, B) Kinetics of mature miR-4306 and pri-miR-4306 expression after treatment of HCAECs/HMDMs with 0, 10, 20, and 40 μg/mL HM-EVs/EC-EVs. (n = 4). (C, D) HM-EV/EC-EV-dependent induction of miR-4306 was resistant to Act D pretreatment of HCAECs/HMDMs. Expression of TNF-α, a short-lived transcript, was reduced in Act D-treated cells (n = 4). $^{*}p < 0.05$. EV: extracellular vesicle; HCAECs: human coronary artery vascular endothelial cells; HM: human monocyte; HMDMs: human monocyte-derived macrophages; miRNA: microRNA; EC: endothelial cell; Act D: actinomycin D; TNF-α: tumor necrosis factor-α.

after incubation with the HM-EVs or EC-EVs for 12 hours compared with before incubation (Figure 6A, B, $p < 0.01$). Additionally, with increasing EV concentrations, a dose-dependent increase in miR-4306 in HCAECs and HMDMs was observed (Figure 6A, B, both $p < 0.01$). We then knocked down miR-4306 expression in HCAECs and HMDMs, which resulted in significantly lower miR-4306 levels in HM-EVs and EC-EVs (Supplementary Figure 3A, $p < 0.01$; Supplementary Figure 4A, $p < 0.01$). Additionally, pre-miR-4306 levels in recipient HCAECs and HMDMs were not altered by incubation with either HM-EVs or EC-EVs (Figure 6A, B). This finding indicated that the increase in miR-4306 level in cells was not due to *de novo* microRNA biosynthesis, but was directly derived from delivery by EVs. We also pretreated HCAECs and HMDMs with the

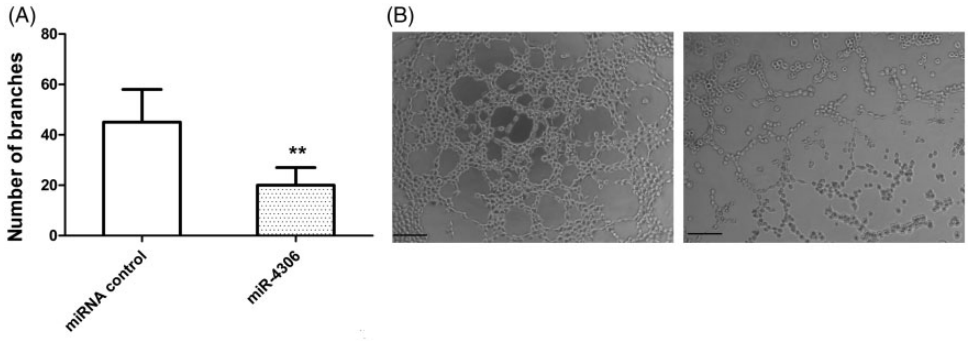

Figure 7. miR-4306 inhibited angiogenesis *in vitro* and *in vivo*. (A, B) miR-4306 inhibited capillary tubule formation of HCAECs. $^{**}p < 0.01$. miRNA: microRNA; HCAECs: human coronary artery vascular endothelial cells.

transcriptional inhibitor actinomycin D and found that induction of miR-4306 was not changed by actinomycin D treatment (Figure 6C, D). This finding indicated that the HM-EV/EC-EV-mediated induction of miR-4306 did not require transcription.

miR-4306 derived from ox-LDL-stimulated HM-EVs inhibits capillary tubule formation of HCAECs through the VEGFA/Akt/NF-κB signaling pathway

We found significantly higher HM-EV-contained miR-4306 levels after HMDM activation with ox-LDL compared with baseline ($p < 0.01$, Supplementary Figure 3b). We then assessed whether miR-4306 can inhibit the proliferation, migration, and angiogenesis of HCAECs. HCAECs were transfected with miR-4306 mimics (Supplementary Figure 3C). We found that overexpression of miR-4306 only slightly suppressed (non-significant) proliferation and migration of HCAECs (Supplementary Figure 5A–D). However, capillary tubule formation of HCAECs was markedly inhibited by miR-4306 mimics ($p < 0.01$ versus miRNA control, Figure 7A, B). HM-EVs plus transfection with the miR-4306 inhibitor abolished the inhibitory effects of HM-EVs on capillary tubule formation of HCAECs (Figure 2D, $p < 0.05$; Figure 2F-d, $p < 0.01$).

According to the miRBase Target database (http://www.mirbase.org), we speculated that VEGFA was a target gene of miR-4306. To identify direct repression of VEGFA by miR-4306, the VEGFA 3′UTR was cloned into a luciferase reporter plasmid and the resulting plasmid was transfected into 293T cells combined with or without treatment with miR-4306. Luciferase reporter activity was significantly lower following incubation with miR-4306 compared with miRNA control ($p < 0.05$, Figure 8A). VEGFA protein expression in HCAECs transfected with the miR-4306 mimic or incubated with HM-EVs was significantly lower compared with that in controls (Figure 8B, D, both $p < 0.01$). Moreover, we found that VEGFA protein levels in HCAECs treated with HM-EVs from patients with CAD were significantly lower than those in controls (Figure 8C, $p < 0.05$).

VEGFA plays a role in promoting PI3K/Akt-dependent EC angiogenesis.[8] We constructed a VEGFA lentiviral expression vector without 3′-UTR and infected HCAECs. VEGFA expression was restored after VEGFA lentiviral infection (Figure 8D). Akt signaling pathway activation was decreased after miR-4306

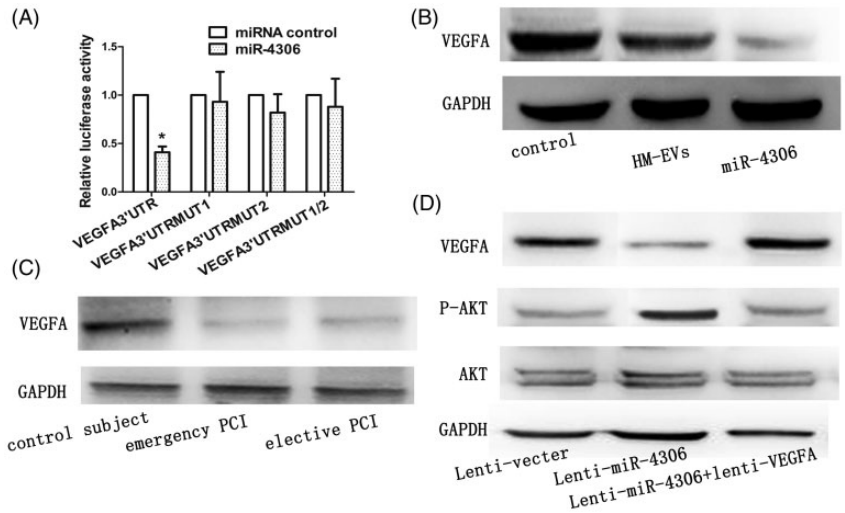

Figure 8. Exogenous miR-4306 delivered by HM-EVs inhibited the VEGFA/Akt signaling pathway in HCAECs. (A) Luciferase activity was analyzed in HEK293 cells 48 hours after transfection. $^{*}p < 0.01$ versus pGL3-VEGFA 3′-UTR-WT. (B) Protein levels of VEGFA in HCAECs after transfection with miR-4306 mimics or HM-EVs. (C) VEGFA protein levels in HMDMs incubated with HM-EVs from patients with elective PCI or patients with emergency PCI. (D) Western blot analysis of VEGFA, (p) Akt, and Akt in HCAECs. HCAECs were cotransduced with lenti-miR-4306, lenti-miR-4306 plus lenti-VEGFA, or a control oligonucleotide ($n = 4$). HM-EVs: human monocyte-extracellular vesicles; VEGFA: vascular endothelial growth factor A; HMDMs: human monocyte-derived macrophages; PCI: percutaneous intervention; HCAECs: human coronary artery vascular endothelial cells.

overexpression. However, miR-4306-mediated inactivation of the Akt signaling pathway was inhibited by VEGFA without 3′-UTR (Figure 8D). Additionally, enhancement of NF-κB signaling by HM-EVs could be abolished by transfecting HM-EV-treated cells with the miR-4306 inhibitor (Figure 4A).

miR-4306 derived from ox-LDL-stimulated EC-EVs enhances lipid accumulation of HMDMs by upregulation of the Akt/NF-κB signaling pathway

HCAEC-released miR-4306 levels were significantly higher after HCAECs were activated with ox-LDL compared with control EVs ($p < 0.01$, Supplementary Figure 4B). We found that miR-4306-transfected cells were more capable of forming foam cells compared with cells in the control group ($p < 0.01$, Supplementary Figure 4C; Figure 9A, B; Table 2). Transfection with the miR-4306 inhibitor could partly abolish enhancement of lipid accumulation in HMDMs treated with EC-EVs (Figure 5A, B).

Overexpression of miR-4306 in HMDMs upregulated the Akt signaling pathway and NF-κB activity (Figure 9C, $p < 0.01$ versus the lentivector group; Figure 3B, $p < 0.05$ versus the ox-LDL group). At the same time, transfection with the miR-4306 inhibitor abrogated the improvement in NF-kB signaling in cells treated with EC-EVs (Figure 3B).

Discussion

In the current study, we observed that HM-EV-derived miRNA-4306 expression was

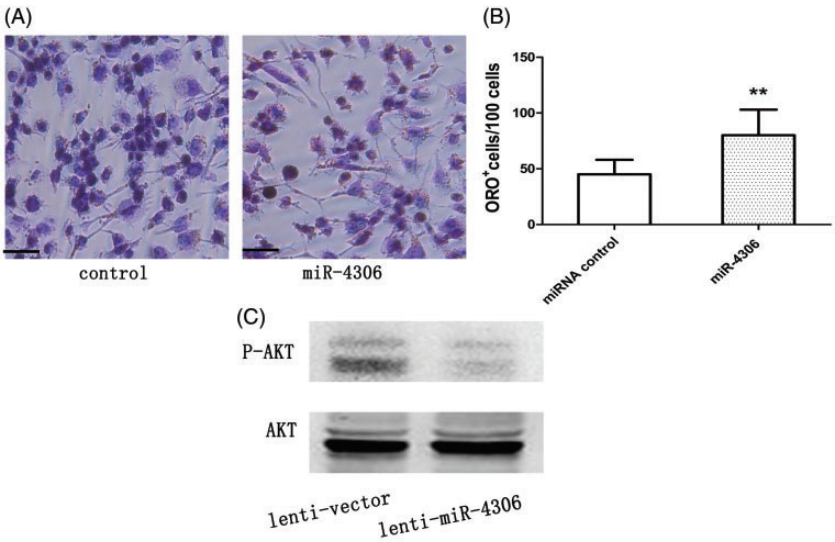

Figure 9. miR-4306 promoted cellular lipid accumulation *in vitro* and *in vivo*. (A, B) miR-4306 enhanced lipid accumulation in HMDMs. Scale bar, 100 μm. (C) miR-4306 upregulated Akt activity in HCAECs (n = 5–6 per group). $^{**}p < 0.01$. miRNA: microRNA; HMDMs: human monocyte-derived macrophages; HCAECs: human coronary artery vascular endothelial cells.

significantly upregulated in CAD. Stimulation by ox-LDL in HM-EV-derived miR-4306 inhibited the angiogenesis ability of HCAECs *in vitro*. However, ox-LDL-stimulated EC-EV-derived miR-4306 enhanced lipid formation in HMDMs.

EVs are released in biological fluids under basal conditions and in pathological settings. Circulating levels of EVs of different cellular origins are increased in cardiovascular diseases and in various conditions associated with cardiovascular risk,[9] including smoking,[10] dyslipidemia,[11] diabetes mellitus,[12] and hypertension.[13] Consistent with these results, we found that HM-EV levels were significantly increased in CAD. We also found that EV levels in ox-LDL-stimulated HMDMs and HCAECs were markedly higher compared with basal levels. Although miRNA profiles of EVs are significantly different from those of their maternal cells,[7] we observed that high expression of miR-4306 was decreased in HCAECs and HMDMs when exposed to ox-LDL. This finding suggests that the same miRNAs can be present in similar proinflammatory situations, regardless of the cells of origin.

Recent studies have indicated that EVs isolated from healthy individuals or EVs released under normal *in vitro* conditions have no effects on cellular function.[14,15] Our results are in agreement with these previous reports. The angiogenesis abilities of HCAECs and lipid formation of HMDMs did not change when cells were cocultured with EVs from unstimulated cells or from control individuals. Our results indicated that EVs from ox-LDL-stimulated HMDMs dramatically inhibited proliferation, migration, and capillary tubule formation of HCAECs. However, HM-EV-contained miR-4306 suppressed the angiogenesis abilities of HCAECs. The effect of factors other than HM-EV-derived miR-4306 on proliferation and migration of HCAECs cannot be excluded. Indeed, most vesicle isolation procedures

that concentrate proteins together with vesicles and subsequent affinity separation have shown that different patterns of miRNAs are associated with either vesicles or with the protein fraction.[16,17] Additionally, Cavallari et al.[18] reported that human serum-derived EVs from healthy blood donors affected vascular remodeling and prevented muscle damage in acute hind limb ischemia. In our study, EVs were from patients with or without CAD. Serum-derived EVs are heterogeneous because of their differing cells of origin (platelets, endothelial cells, or monocytes/leukocytes). Platelets are major sources of serum-derived EVs in the peripheral bloodstream and approximately two thirds of serum-derived EVs are derived from platelets.[19] Serum-derived EVs from various cells might play different roles in the same disease.

EVs are present not only near the activated parental cell, but also readily circulate in the vasculature. Both mechanisms allow for signaling not only to neighboring cells, but also to cells at a remarkable distance from their donor cell origin.[20] Our study showed that *in vitro*, EVs from ox-LDL-stimulated HMDMs suppressed proliferation, migration, and capillary tubule formation of HCAECs. However, EVs from ox-LDL-stimulated HCAECs suppressed lipid accumulation in HMDMs. Further analysis showed that EV-contained miR-4306 played a vital role in this process. We speculate that there is bidirectional exchange of genetic information between HMDMs and HCAECs through EVs transferring selected patterns of miRNAs.

EVs play an important role in pathophysiological processes of atherosclerosis by accelerating plaque formation, intravascular calcifications, unstable plaque rupture, and thrombus formation.[6] Hutter et al.[21] reported that ox-LDL intensely induced VEGF production in monocytes and markedly elevated tube formation in cocultured endothelial cells. Our findings suggest that the mechanism for capillary tubule and lipid formation in vascular ECs and macrophages is partly due to miR-4306 regulating the VEGFA/Akt/NF-κB signaling pathway. EVs of various cellular origins can induce foam cell formation by enhancing lipid and cholesterol accumulation in macrophages.[22] Foam cell formation could be mediated by SR-A and low-density lipoprotein receptor-1 by facilitation of uptake of modified lipids.[23] We found that ox-LDL-stimulated EC-EV-derived miR-4306 enhanced lipid accumulation of HMDMs by upregulation of the Akt/NF-κB signaling pathway.

Conclusions

In summary, our study shows that EVs from ox-LDL-stimulated HMDMs inhibit capillary tubule formation of HCAECs and EVs from ox-LDL-stimulated HCAECs promote lipid accumulation in HMDMs. The possible mechanism of these findings is partly due to miR-4306 upregulation of the Akt/NF-κB signaling pathway during this process. This paracrine cellular crosstalk between HCAECs and HMDMs probably supports the pro-atherosclerotic effects of EVs under ox-LDL stress.

Declaration of conflicting interest

The authors declare that there is no conflict of interest.

Funding

This work was supported by a General Financial Grant from the Science and Technology Department of Sichuan Province (grant number: 2016JY0172, Chengdu, China), a General Financial Grant from the Education Department of Sichuan Province (grant number: 17ZB0168, Chengdu, China), and a

General Financial Grant from the China Postdoctoral Science Foundation (grant number: 2016M592678, Beijing, China).

References

1. Li J, Tan S, Kooger R, et al. MicroRNAs as novel biological targets for detection and regulation. *Chem Soc Rev* 2014; 43: 506–517.
2. Karakas M, Schulte C, Appelbaum S, et al. Circulating microRNAs strongly predict cardiovascular death in patients with coronary artery disease-results from the large AtheroGene study. *Eur Heart J* 2017; 38: 516–523.
3. Boon RA. Endothelial microRNA tells smooth muscle cells to proliferate. *Circ Res* 2013; 113: 7–8.
4. Pan Y, Liang H, Liu H, et al. Platelet-secreted microRNA-223 promotes endothelial cell apoptosis induced by advanced glycation end products via targeting the insulin-like growth factor 1 receptor. *J Immunol* 2014; 192: 437–446.
5. Lo Cicero A, Stahl PD and Raposo G. Extracellular vesicles shuffling intercellular messages: for good or for bad. *Curr Opin Cell Biol* 2015; 35: 69–77.
6. Boulanger CM, Loyer X, Rautou PE, et al. Extracellular vesicles in coronary artery disease. *Nat Rev Cardiol* 2017; 14: 259–272.
7. Diehl P, Fricke A, Sander L, et al. Microparticles: major transport vehicles for distinct microRNAs in circulation. *Cardiovasc Res* 2012; 93: 633–644.
8. Merckx J, Wali R, Schiller I, et al. Diagnostic accuracy of novel and traditional rapid tests for influenza infection compared with reverse transcriptase polymerase chain reaction: a systematic review and meta-analysis. *Ann Intern Med* 2017; 167: 394–409.
9. Potente M and Carmeliet P. The link between angiogenesis and endothelial metabolism. *Annu Rev Physiol* 2017; 79: 43–66.
10. Amabile N, Cheng S, Renard JM, et al. Association of circulating endothelial microparticles with cardiometabolic risk factors in the Framingham heart study. *Eur Heart J* 2014; 35: 2972–2979.
11. Li CJ, Liu Y, Chen Y, et al. Novel proteolytic microvesicles released from human macrophages after exposure to tobacco smoke. *Am J Pathol* 2013; 182: 1552–1562.
12. Koga H, Sugiyama S, Kugiyama K, et al. Elevated levels of remnant lipoproteins are associated with plasma platelet microparticles in patients with type-2 diabetes mellitus without obstructive coronary artery disease. *Eur Heart J* 2006; 27: 817–823.
13. Koga H, Sugiyama S, Kugiyama K, et al. Elevated levels of VE-cadherin-positive endothelial microparticles in patients with type 2 diabetes mellitus and coronary artery disease. *J Am Coll Cardiol* 2005; 45: 1622–1630.
14. Nomura S, Shouzu A, Omoto S, et al. Effects of losartan and simvastatin on monocyte-derived microparticles in hypertensive patients with and without type 2 diabetes mellitus. *Clin Appl Thromb Hemost* 2004; 10: 133–141.
15. Berezin AE, Kremzer AA, Martovitskaya YV, et al. Pattern of endothelial progenitor cells and apoptotic endothelial cell-derived microparticles in chronic heart failure patients with preserved and reduced left ventricular ejection fraction. *EBioMedicine* 2016; 4: 86–94.
16. Jansen F, Yang X, Franklin BS, et al. High glucose condition increases NADPH oxidase activity in endothelial microparticles that promote vascular inflammation. *Cardiovasc Res* 2013; 98: 94–106.
17. Boing AN, van der Pol E, Grootemaat AE, et al. Single-step isolation of extracellular vesicles by size-exclusion chromatography. *J Extracell Vesicles* 2014; 3–10.
18. Nordin JZ, Lee Y, Vader P, et al. Ultrafiltration with size-exclusion liquid chromatography for high yield isolation of extracellular vesicles preserving intact biophysical and functional properties. *Nanomedicine* 2015; 11: 879–883.
19. Cavallari C, Ranghino A, Tapparo M, et al. Serum-derived extracellular vesicles (EVs) impact on vascular remodeling and prevent muscle damage in acute hind limb ischemia. *Sci Rep* 2017; 7: 8180.
20. Hunter MP, Ismail N, Zhang X, et al. Detection of microRNA expression in

human peripheral blood microvesicles. *PLoS One* 2008; 3: e3694.
21. Mause SF and Weber C. Microparticles: protagonists of a novel communication network for intercellular information exchange. *Circ Res* 2010; 107: 1047–1057.
22. Hutter R, Speidl WS, Valdiviezo C, et al. Macrophages transmit potent proangiogenic effects of oxLDL in vitro and in vivo involving HIF-1alpha activation: a novel aspect of angiogenesis in atherosclerosis. *J Cardiovasc Transl Res* 2013; 6: 558–569.
23. Keyel PA, Tkacheva OA, Larregina AT, et al. Coordinate stimulation of macrophages by microparticles and TLR ligands induces foam cell formation. *J Immunol* 2012; 189: 4621–4629.
24. Zhu X, Ng HP, Lai YC, et al. Scavenger receptor function of mouse Fcgamma receptor III contributes to progression of atherosclerosis in apolipoprotein E hyperlipidemic mice. *J Immunol* 2014; 193: 2483–2495.